Recirculator system for the MRT

When I tinker with my wireless set

I realize that all the sounds in the world

are in my room.

George Bernard Shaw

Chapter 3

RECIRCULATOR SYSTEM FOR THE MRT

In this chapter, we discuss the effect of bandwidth decorrelation, also known as chromatic aberration, in the image. A recirculator system was designed and built to overcome the effects of bandwidth decorrelation. The design criteria for the recirculator and other hardware developed are also described.

3.1 Effects of bandwidth

Although the use of larger bandwidths results in a better sensitivity of a telescope, it restricts the angular range over which an image can be made if the relative delays between the signals being correlated are not compensated. This effect known as bandwidth decorrelation is also referred to by other names like chromatic aberration and fringe washing. This effect mainly results from the variation of the relative phase difference between the correlator inputs as a function of frequency within the observing bandwidth. If the relative delay is large, the signals at one end of the band may be interfering destructively while the signals at the other end of the band are interfering constructively. This results in the diminution of the interferometer response, i.e., the fringe contrast is reduced. If the differential delay is greater than the coherence time,

then the two signals can no longer interfere constructively. The coherence time is of the order of the inverse of the bandwidth and depends on the band-shape.

We now analyze bandwidth decorrelation more quantitatively by looking at the relationship between visibility and brightness given by Equation 1.1[1]:

$$\frac{A_N(\xi,\eta)B(\xi,\eta)}{\sqrt{1-\xi^2-\eta^2}} = \int\int V(x,y)e^{j2\pi(x\xi+y\eta)}\mathrm{d}x\mathrm{d}y$$

This relationship is true only for a monochromatic signal since the spatial[2] frequencies x and y are frequency dependent terms.

For any frequency, ν, in the passband, the true spatial frequencies x, and y, are related to $x_\circ$ and $y_\circ$, which are the assigned values of x and y corresponding to center frequency of the band, $\nu_\circ$. $(x_\circ, y_\circ)$ in terms of (x,, y,) is given by [16].

$$(x_o, y_o) = \left(\frac{\nu_o}{\nu}x_\nu, \frac{\nu_o}{\nu}y_\nu\right) \tag{3.1}$$

The visibility function $V(x_\nu, \mathrm{y},)$ may be expressed in terms of $V(x_\circ, y_\circ)$ by making a change of variable in the Equation 3.1.

Since $V(x_\nu, \mathrm{y},) \rightleftharpoons B'(\xi,\eta)$ [3], from the similarity theorem we get:

$$V\left(x_\nu\frac{\nu_o}{\nu}, y_\nu\frac{\nu_o}{\nu}\right) \rightleftharpoons \left(\frac{\nu}{\nu_o}\right)^2 B'\left(\xi\frac{\nu}{\nu_o}, \eta\frac{\nu}{\nu_o}\right) \tag{3.2}$$

i.e., if the visibilities were measured on a grid scaled by $\frac{\nu_o}{\nu}$ then the (ξ,η) grid in the brightness domain would be scaled by $\frac{\nu}{\nu_o}$. Furthermore, the brightness would be scaled by $\left(\frac{\nu}{\nu_o}\right)^2$ to conserve the total integrated flux.

The overall response over the passband is obtained by integrating $B'\left(\xi\frac{\nu}{\nu_o}, \eta\frac{\nu}{\nu_o}\right)$ over the passband with its weighting. This can be thought of as a process of averaging a large number of maps each with a different scale factor $\frac{\nu}{\nu_o}$. All these

[1] We consider only the visibilities measured with a coplanar array for simplicity. The final result is the same for visibilities measured with a non-coplanar array [17].

[2] spatial frequency = baseline/wavelength.

[3] $B'(\xi,\eta) = \frac{A(\xi,\eta)B(\xi,\eta)}{\sqrt{1-\xi^2-\eta^2}}$

maps are aligned at the delay center, i.e., ($\xi = 0,\ \eta = 0$) and get misaligned as one moves away from the delay center, i.e., at larger ξ and η. The effect is to produce a radial smearing of the brightness distribution. The smeared brightness is then convolved with the beam $b_o(\xi,\eta)$, the synthesized beam corresponding to the center frequency ν_o. Thus, the measured brightness over the passband $B_{\Delta\nu}(\xi,\eta)$ may be expressed as:

$$B_{\Delta\nu}(\xi,\eta) = \frac{\int_0^\infty H(\nu)\left(\frac{\nu}{\nu_o}\right)^2 B\left(\xi\frac{\nu}{\nu_o}, \eta\frac{\nu}{\nu_o}\right) d\nu}{\int_0^\infty H(\nu)d\nu} \star\star\, b_o(\xi,\eta) \tag{3.3}$$

where

$\star\star$ represents a two-dimensional convolution.

$B_{\Delta\nu}(\xi,\eta)$ is the measured brightness distribution due to observing with a passband.

$H(\nu)$ is the power spectrum of the passband and is assumed to be identical for all antennas.

$b_o(\xi,\eta)$ is the synthesized beam corresponding to the center frequency ν_o. The beam does not vary with frequency because the same transfer function $W(x,\mathrm{y})$ is used to represent the whole frequency passband.

In terms of visibilities measured for a point source, the interferometer response at a single frequency may be written as $V(x,\mathrm{y},z),\ = V_{pt}e^{j2\pi\nu\tau(x,y,z)}$ where $\tau(x,\mathrm{y},z) = \frac{x\lambda}{c}\xi + \frac{y\lambda}{c}\eta + \frac{z\lambda}{c}\zeta$ and V_{pt} is the strength of the point source.

The response of an interferometer, $V_{\Delta\nu}(x,\mathrm{y},\mathrm{z})$, to a point source over a

passband, $H(\nu)$, centered at ν_o is obtained by integrating the point source response at a single frequency over the passband.

$$V(x,y,z)_{\Delta\nu} = \frac{V_{pt}}{\int H(\nu)\mathrm{d}\nu}\int H(\nu) * \delta(\nu_o)e^{j2\pi\nu\tau(x,y,z)}d\nu \tag{3.4}$$

The integral on the RHS is the Fourier transform of the convolution[4] of H(v) and $\delta(\nu_o)$, therefore

$$V(x,y,z)_{\Delta\nu} = \mathcal{F}(H(\nu))\frac{V_{pt}}{\int H(\nu)\mathrm{d}\nu}e^{j2\pi\nu_o\tau(x,y,z)} = \gamma(\tau(x,y,z))V(x,y,z)_{\nu=\nu_o} \tag{3.5}$$

where $\gamma(\tau(x,y,z)) = \frac{\mathcal{F}(H(\nu))}{\int H(\nu)\mathrm{d}\nu}$ is the bandwidth decorrelation term.

For a rectangular band from $\left(\nu_o - \frac{\Delta\nu}{2}\right)$ to $\left(\nu_o + \frac{\Delta\nu}{2}\right)$

$$V(x,y,z)_{\Delta\nu} = \frac{V_{pt}}{\Delta\nu}\left(\frac{\sin(\pi\Delta\nu\tau)}{\pi\Delta\nu\tau}\right)e^{j2\pi\nu_o\tau(x,y,z)} = \left(\frac{\sin(\pi\Delta\nu\tau)}{\pi\Delta\nu\tau}\right)V(x,y,z)_{\nu=\nu_o} \tag{3.6}$$

The response of an interferometer to a point source is modified by a multiplication term which is the Fourier transform of the bandpass. This causes a loss in sensitivity for large delays, τ in the above equation, resulting in the signal from these directions to be decorrelated. For a given source, visibilities on different baselines suffer from different amounts of decorrelation. The observed visibilities at different baselines appear to be effectively reduced by a factor $sinc(\Delta\nu\tau)$, since τ increases with the baseline length. This causes distortion or smearing of the image particularly at large delays.

To reduce decorrelation in a given direction, we need to compensate for the geometric delay in that direction. This is done by introducing a delay in the path of one of the antennas of the interferometer. A delay compensated interferometer is shown in Figure 3.1.

[4] $f(t) * g(t) \rightleftharpoons F(\nu)G(\nu)$

The east-west group has a narrow primary beam of two degrees in RA. At the MRT, we use a bandwidth of 1 MHz. This does not pose a problem for synthesizing the primary beam in this direction. However both the east-west and the north-south groups have wide primary beams in declination extending from $-70°$ to $-10°$. We will, therefore, be concerned with compensating geometric delays for zenith angles along the meridian $za_\circ$. The delay can be compensated for a zenith angle along the meridian, $za'_\circ$, by introducing a delay of $\frac{y\lambda \sin(za'_\circ)}{c}$ where y is the baseline (in wavelengths) along the north-south arm. The correlation response around this point in declination is then graded by $sinc(\Delta\nu\Delta\tau)$ where $\Delta\tau$ is the uncompensated delay given as $\mathrm{A}\tau = \frac{y\lambda}{c}\left(\sin(za_\circ) - \sin(za'_\circ)\right)$ and the grading function (delay beam) is $sinc\left(\Delta\nu\left(\frac{y\lambda \sin(za_\circ)}{c} - \frac{y\lambda \sin(za'_\circ)}{c}\right)\right)$. Since the delays are a function of sine of the zenith angle, the rate of change of decorrelation is slower at larger zenith angles and therefore the delay beams are broader around larger $za_\circ$. For a given delay compensation, we will be able to observe a part of the sky with small decorrelation. This is referred to as the delay zone around the point at which the geometrical delay has been compensated. At the MRT, our design goal is to keep the bandwidth decorrelation to less than 20% even on the longest north-south baselines. To image the declination range $-70° \leq \delta \leq -10°$ with the MRT, using a 1 MHz band, one requires visibility measurements with four delay settings.

We now discuss the design of a recirculator system built for the MRT to measure, in an optimal way, the visibilities with different delay settings.

3.2 A recirculator system for the MRT

We saw in the previous section that the bandwidth decorrelation limits the angular range over which an image is made. Signals from the region of the sky

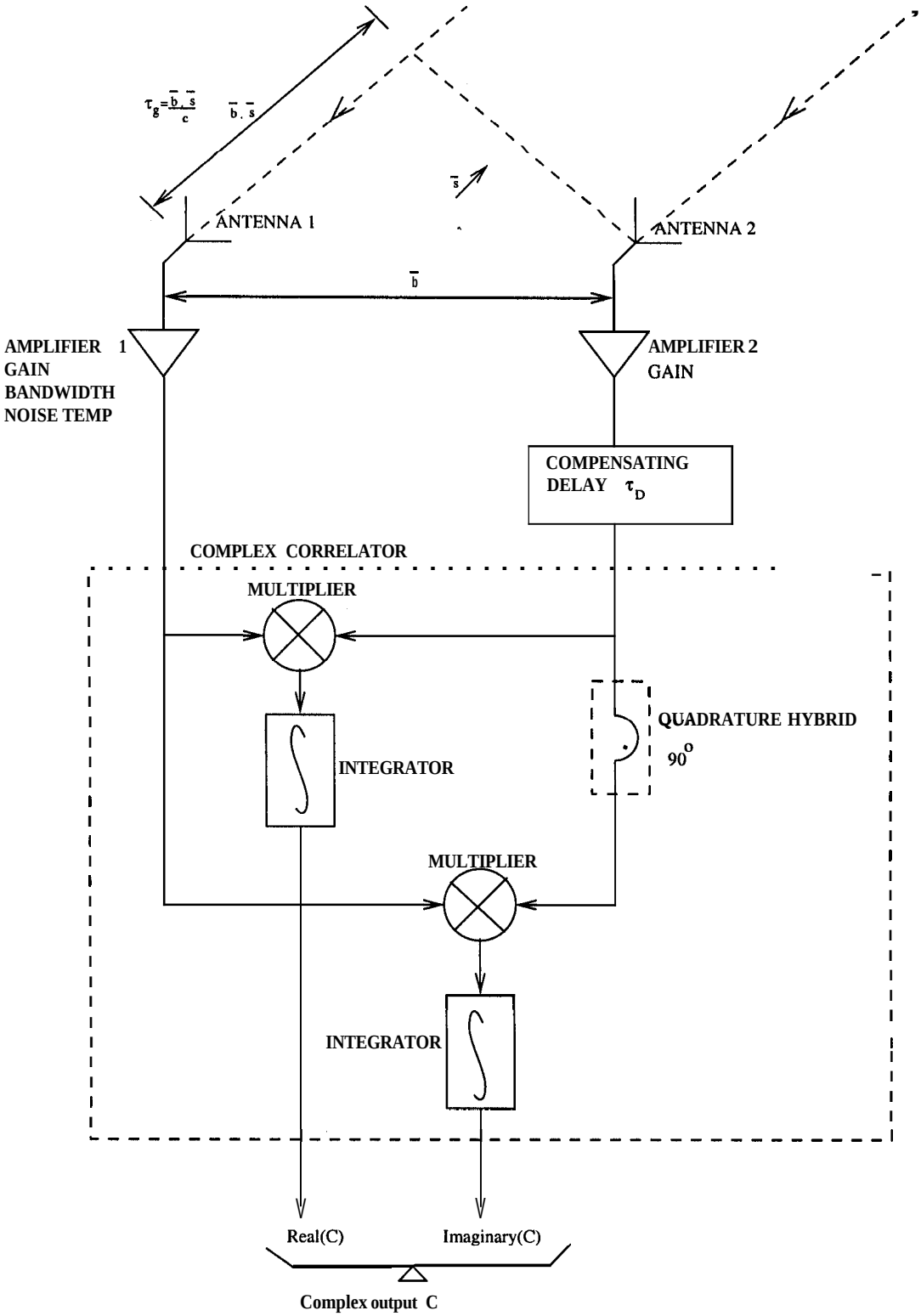

Figure 3.1: A schematic of a delay compensated interferometer

for which the delay between the interferometer elements is uncompensated get decorrelated and the image gets distorted when finite bandwidth is used. To reduce this bandwidth decorrelation, we need to compensate for the delays. The number of delays required depends on the angular coverage required and on how much deterioration in sensitivity we are willing to tolerate in an image. As mentioned earlier, with each delay a part of the sky referred to as a delay zone can be imaged.

3.2.1 Need for a recirculator system

We consider a few possible methods of measuring visibilities with different delay settings, using the existing 512 channel complex correlator system which can work with a maximum clock frequency of 12 MHz.

(a) Collect data for each delay zone on separate days. In doing so the number of days required to collect a set of data would increase thereby reducing the surveying sensitivity[5]. We observe each allocation for 2-3 days to be able to get interference free data. Furthermore, we re-observe with a gap of about 6 months to image regions corrupted by the Sun (Section 2.3). Collecting data for different zones on separate days makes the total time required to be very large. For a bandwidth of 1 MHz, we need to collect data from four delay zones and therefore the total observing time required would be of the order of four years[6] assuming zero down-time of the telescope. Also, because of paucity of suitable calibrators in the field of

[5]Surveying sensitivity is the minimum flux density detectable in a survey of a particular region when the whole survey is completed in a total time t_s seconds. The sensitivity is expressed in terms of t_s rather than t, the time spent on the measurement in any one particular direction.

[6]60 days(to cover 880 m)*4(delay zones)*3(for interference)*2(for the Sun)=1440 days =4 years

view of the MRT, calibrating the different zones on different days would be a problem (see Section 4.2 for more details).

(b) Share the time to observe with different delay settings. The resolution of the MRT is about 4' corresponding to 16 seconds of time for a source on the equator. Therefore, the visibilities can be measured by time multiplexing, i.e., by measuring visibilities for each delay setting for $\frac{16}{N}$ seconds. N being the number of delays required. This way we get data for all the declinations in a single day. This however results in a loss in sensitivity[7] by $\sqrt{N}$ for N delay settings.

(c) To overcome the problems in the above schemes, there is a need for a system which will allow data to be collected for each zone without degradation in sensitivity and will also allow the visibilities with different delays to be measured in the same day. This requires a system which would store the samples for T seconds followed by a correlator system that would measure visibilities with each delay setting in $\frac{T}{N}$ seconds. Such a system wherein the data is sampled and stored at a slower rate and then processed N times at a faster rate is called a recirculator. To implement this, a dual-buffer memory system is employed between the sampler and the correlator. The data from the sampler is stored at a given rate in one bank while the data from the other bank is read and processed N times faster in the correlator. Figure 3.2 represents the basic principle of a recirculator system.

[7] We neglect the component of noise due to confusion (defined in chapter 2) which is independent of the integration used.

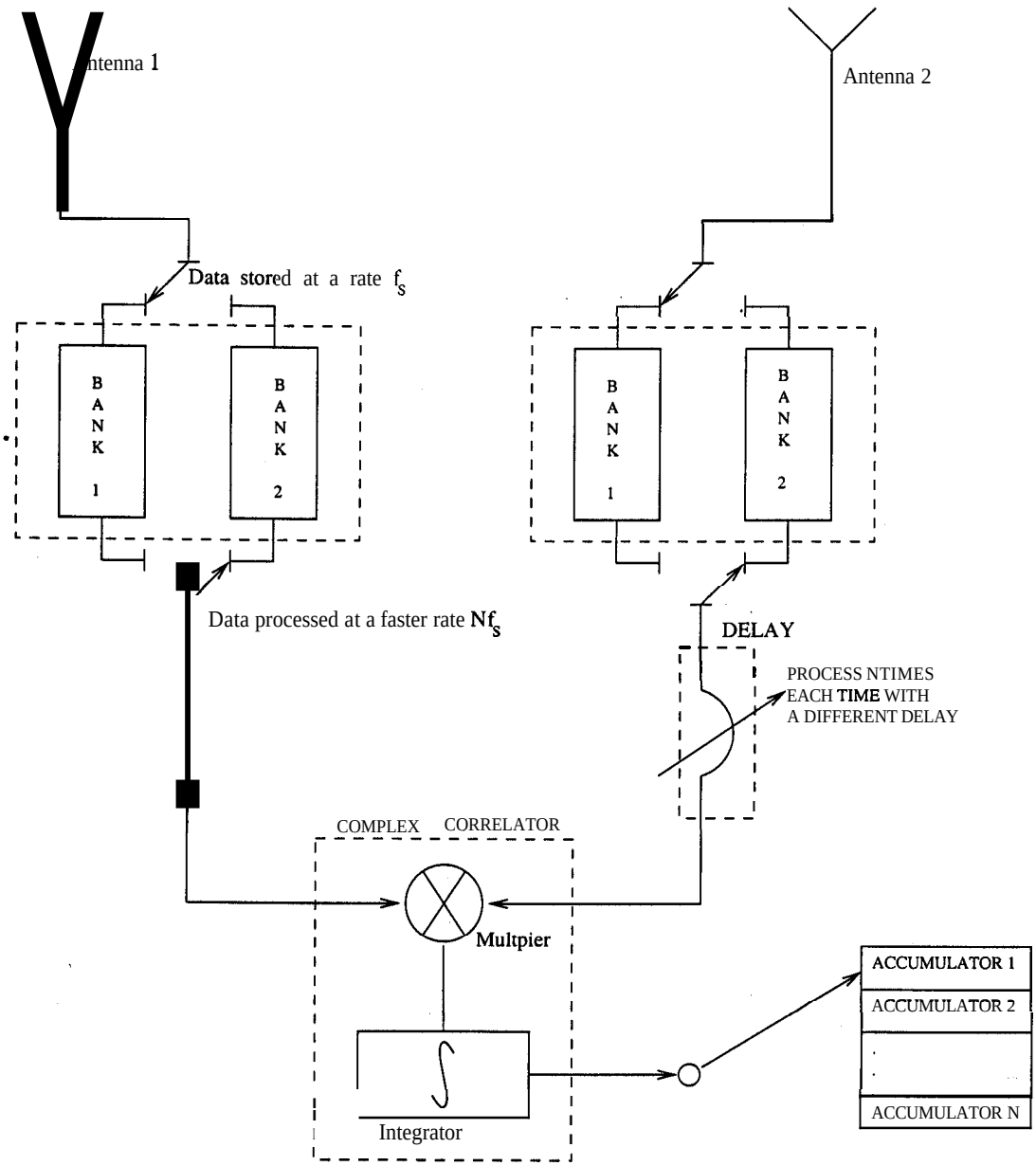

Figure **3.2:** Schematic showing the basic principle of a recirculator. Data is stored at a rate f_s in a dual-buffer memory and is read out and processed at a rate Nf_s in the correlator, allowing data to be processed N times, each time with a different delay compensation.

3.2.2 Design Criterion

The MRT receiver system provides an option of using **3.0** MHz, **1.5** MHz, **1** MHz and **0.15** MHz bandwidths. One would generally be interested in using the widest band available for more sensitivity. Higher sensitivity would also improve our calibration because we would be able to use weaker and therefore more number of sources for calibration. However, for wide field imaging the bandwidth decorrelation effect (described in the previous section) becomes more severe. Thus, a larger bandwidth would imply measurements of correlations at a larger number of delays to cover a large field of view.

In this section we discuss the choice of bandwidth used, the sampling frequency employed and the size of memory buffers used, and discuss the specifications and criteria for the design of a data acquisition system.

3.2.2.1 Choice of bandwidth

We begin by determining an appropriate bandwidth for use to maximize surveying sensitivity, given that we intend to map 60° of the sky using a correlator system which can work with clock rates of up to 12 MHz. Furthermore, we start with a design goal of letting the maximum loss due to bandwidth decorrelation to be 20% on the longest baseline.

The surveying sensitivity, SS_{min}, is defined as:

$$SS_{min} = \sqrt{N_D} f_{os} \frac{\sqrt{2}\, 2k_B(\sqrt{T_{sys_{ew}} T_{sys_{ns}}})}{\sqrt{N_b} A_e \sqrt{\Delta\nu t}} \tag{3.7}$$

where f_{os} is the degradation factor for the digital correlator and N_D is the number of days required to cover the complete zenith angle range. N_D is given

by:

$$N_D \geq int\left(\frac{N_{zn}}{N_{del}}\right) \tag{3.8}$$

where N_{zn} is the number of delay settings needed to cover the required zenith angle range and N_{del} is the number of delays with which the correlations can be measured using a correlator system that can run up to a maximum frequency of f_{corr}^{max}.

N_{zn} depends on the delay range of interest, τ_{range}, and the maximum allowed decorrelation loss, x_{max}, and may be expressed as

$$N_{zn} \geq int\left(\frac{\tau_{range}\Delta\nu}{2sinc^{-1}(1-x_{max})}\right) \tag{3.9}$$

while N_{del} is given by

$$N_{del} \leq int\left(\frac{f_{corr}^{max}}{2\Delta\nu\ os}\right) \tag{3.10}$$

where os is the oversampling factor and $\Delta\nu$ is the bandwidth used.

We therefore note that for a given array, the surveying sensitivity depends upon the following:

(a) the bandwidth used (Av).

(b) the delay range to be imaged (τ_{range}).

(c) the maximum decorrelation allowed (x_{max}).

(d) the maximum clock speed at which the correlator works (f_{corr}^{max}).

(e) the oversampling factor (os) and the degradation factor f_{os}.

The following have to be considered in obtaining an optimal surveying sensitivity.

[a]The sensitivity obtainable increases as the square-root of the bandwidth. However, the number of days required may increase with the bandwidth. These two factors affect the surveying sensitivity contrarily.

[b]The sampling frequency has to be set considering

(i) the bandpass sampling criterion.

(ii) that the harmonics of the sampling clock should not fall inside the RF and first IF bands because these can cause spurious correlations.

[c] The sensitivity also increases to a certain extent with larger oversampling factor for correlators with limited number of bits. However, a larger oversampling factor could reduce the number of delays covered with recirculation for a given correlator speed. This would increase the number of days required, and hence, reduce the surveying sensitivity.

Let us look at items [b] and [c] in more detail:

- The permissible sampling frequencies, f_s, for bandpass signals.

  For a bandpass signal, we need to sample keeping in mind the criterion for bandpass or harmonic sampling.

  The permissible sampling frequencies for a bandpass signal must satisfy the following criterion to avoid loss in sensitivity due to aliasing [35].

$$\frac{2}{n}\frac{f_h}{(f_h - f_l)} \leq \frac{f_s}{(f_h - f_l)} \leq \frac{2}{n-1}\left(\frac{f_h}{(f_h - f_l)} - 1\right) \qquad (3.11)$$

  where n is an integer such that $1 \leq n \leq \frac{f_h}{f_h - f_l}$, f_h is the highest frequency in the bandpass and f_l is the lowest frequency in the bandpass. In Figure 3.3 the permissible sampling rates are shown as clear areas and sampling frequencies not permissible are shown as shaded areas.

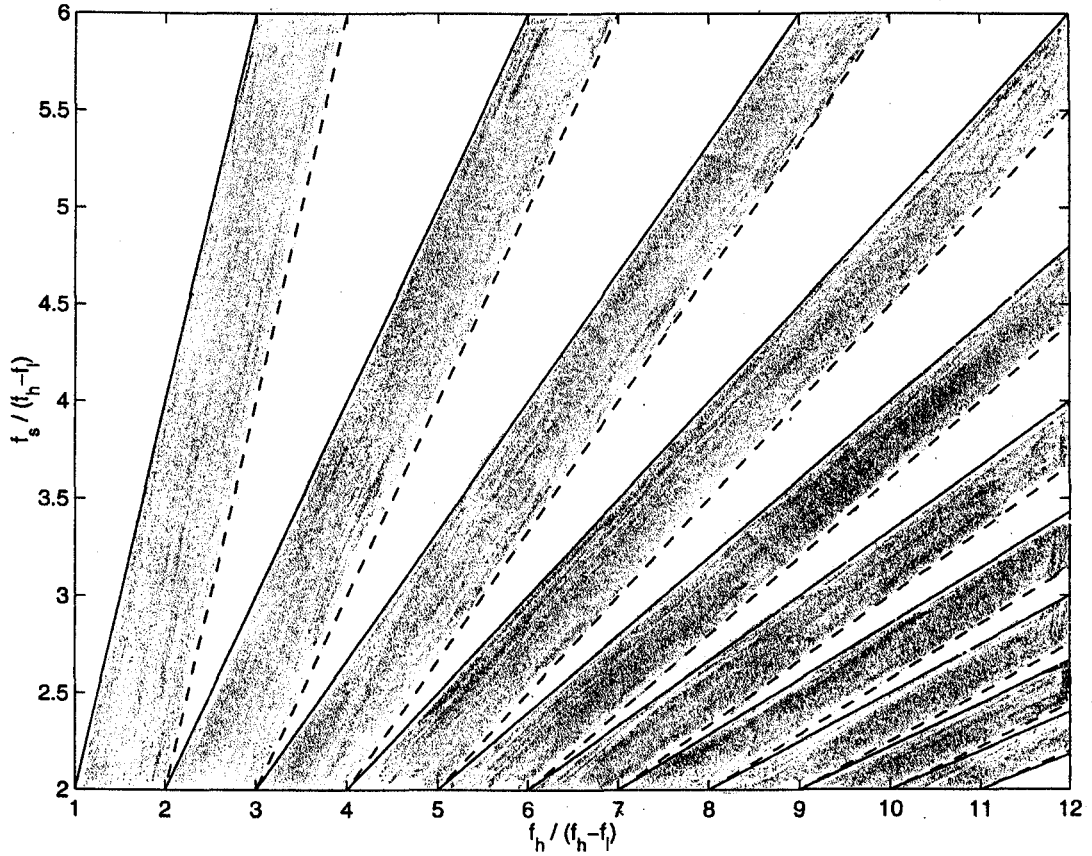

Figure 3.3: Bandpass sampling criteria: Clear areas show permissible sampling regions.

- The sampling frequencies that do not have harmonics in the RF (151.5 MHz) and first IF (30 MHz) signal bands.

  The basic system clock may have to be adjusted so that the harmonics of the sampling clock and other clocks used in the system do not fall in the 1 MHz bands about 151.5 MHz and **30** MHz. Harmonic pick-ups on the IF path (30 MHz) which vary faster than the LO switching period would cause spurious correlations and therefore need to be also considered. The duty cycle of the sampling clock also needs to be taken into account because the harmonic contents of the sampling clock depends on it.

- Dependence of sensitivity on the oversampling factor.

  Signals represented by limited bit quantization result in a loss in sensitivity compared to that of an unquantized (analog) correlator. A band-limited signal that is quantized results in the generation of new frequency components in the waveform, so it is no longer band-limited. If it is Sampled at the Nyquist rate corresponding to the unquantized waveform, some information will be lost, and the sensitivity will be less than that for unquantized sampling.

  The dependence of the degradation factor, f_{os}, which is basically the deterioration of sensitivity [1] of a **3** x **3** correlator on the sampling rates is shown in Figure **3.4.**

We now calculate the surveying sensitivity obtainable with the MRT as a function of bandwidth to cover the full 60" $(-70° \leq \delta \leq -10°)$ using a correlator system working at 12 MHz and allowing a maximum decorrelation of 20% on the longest baseline. We normalize the surveying sensitivity with that obtained using a **4** MHz bandwidth which would require 16 days of observations to cover $-70° \leq \delta \leq -10°$ with decorrelation not exceeding 20%. We choose **4** MHz to normalize the surveying sensitivity because this is the maximum bandwidth[8] centered at 10 MHz that we can use with a sampling frequency of 12 MHz. Therefore the normalized surveying sensitivity may be represented as:

$$SS_N = SS_{min} / \left(\frac{1}{1.23} \sqrt{\frac{4 \text{ MHz}}{16 \text{ days}}} \right) \tag{3.12}$$

[8]Note: The 6 MHz can be used only as baseband. We therefore consider only bandwidths centered at 10 MHz. A 4 MHz band centered at 10 MHz is the largest bandwidth usable with a sampling frequency of 12 MHz.

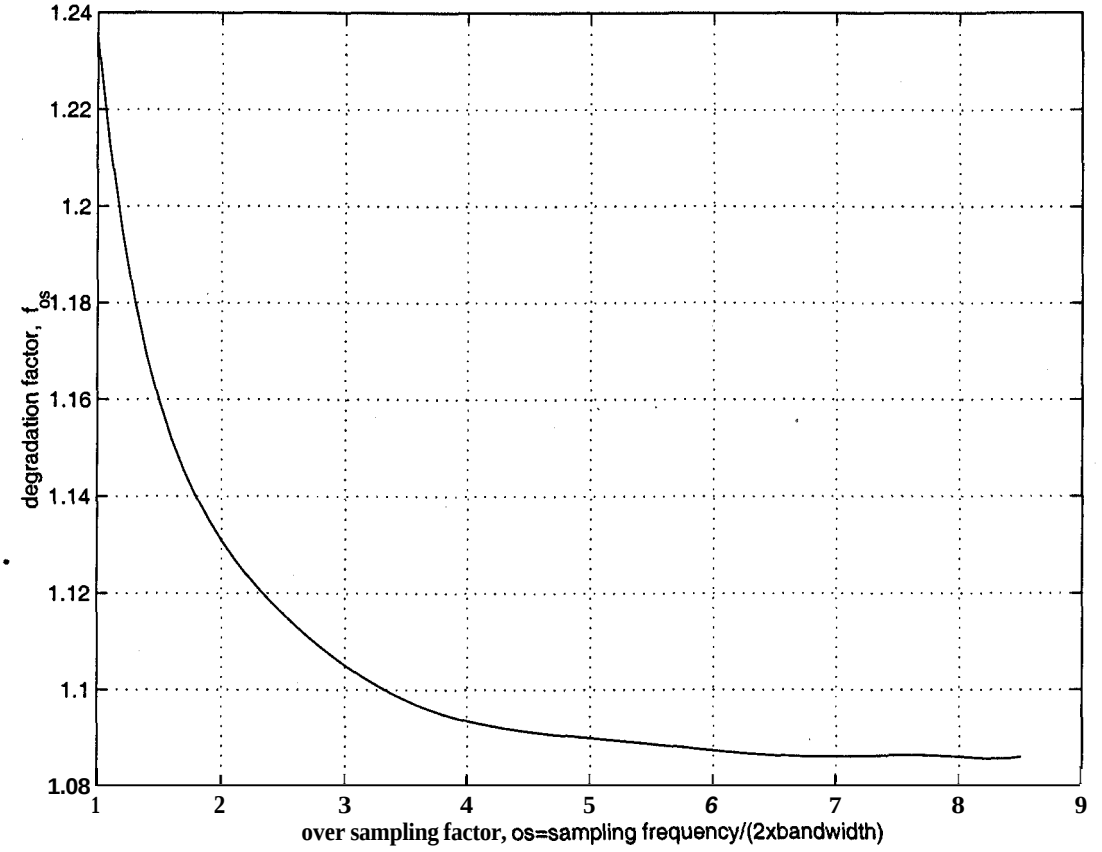

Figure 3.4: Degradation factor, f_{os}, versus over-sampling factor, os, for a 3×3 correlator [1]

where 1.23 is the degradation factor (obtained from Figure 3.4) for an over-sampling factor of 1.009 in a 3x3 correlator system. The plot of number of delay zones required and the number of days needed is shown in Figure 3.5. The plot of normalized surveying sensitivity is shown in Figure 3.6.

The plot of surveying sensitivity against bandwidth is not a smooth curve. This is because at some bandwidths the number of days required to cover the entire declination range changes abruptly. From this plot we find that a bandwidth of about 1.1 MHz gives us the best surveying sensitivity. This requires 4 delay settings ($N_{del} = 4$), one day ($N_D = 1$) and an oversampling factor of 1.08 ($os = 1.08$). The bandwidth which gives surveying sensitivity

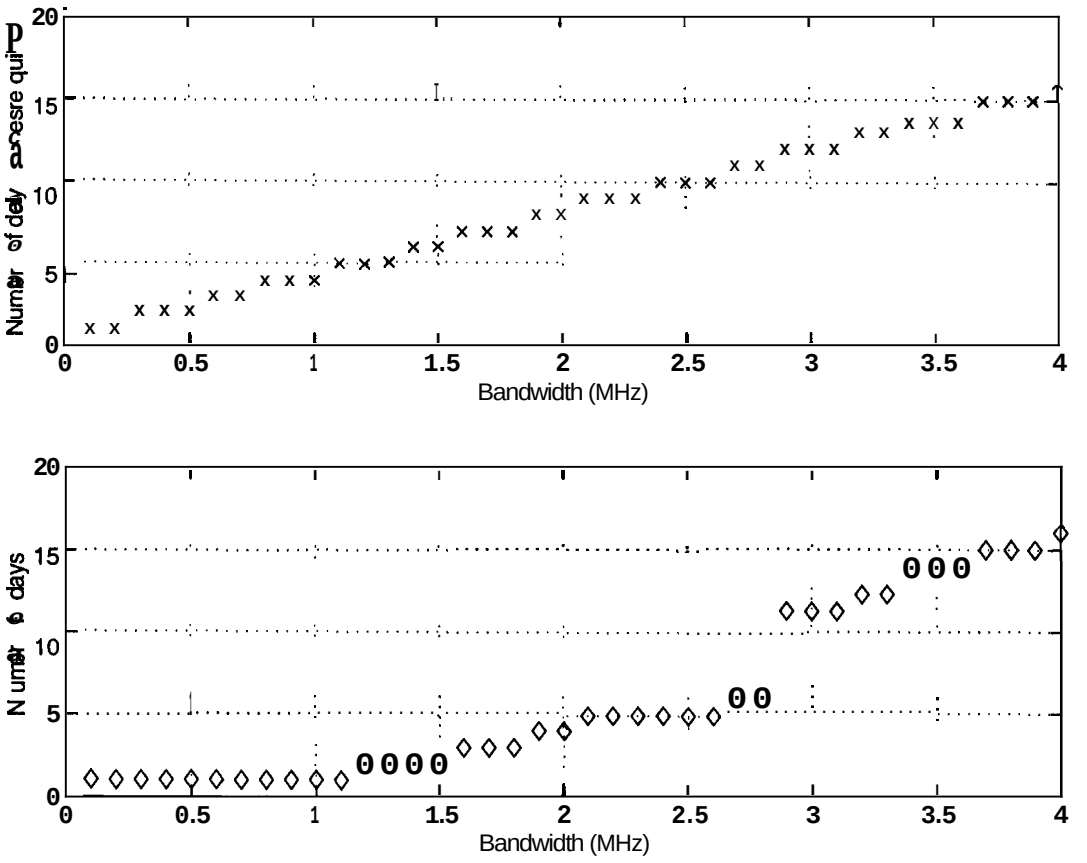

Figure 3.5: This plots show the number of delay zonks required and the number of days needed to cover the declination range $-70° \leq \delta \leq -10°$ with a maximum decorrelation of 20% on the longest baseline.

closest to the above criterion is provided by the 1 MHz filters in the MRT receiver system. So even though the existing system can be used with a 3 MHz bandwidth, for surveying the declination range $-70° \leq \delta \leq -10°$ with the best surveying sensitivity using a 512-channel complex correlator system which can work with a maximum clock frequency of 12 MHz, we use a bandwidth of 1 MHz. Figure 3.7 shows the bandwidth decorrelation for 4 delay settings with trolleys positioned at 880 m for a 1 MHz bandwidth. 880 m being the longest north-south baseline measured, this plot shows the "worst-case", i.e., the maximum decorrelation that we will have in the recirculator mode. The delay beam of the array which takes into consideration all the interferometers

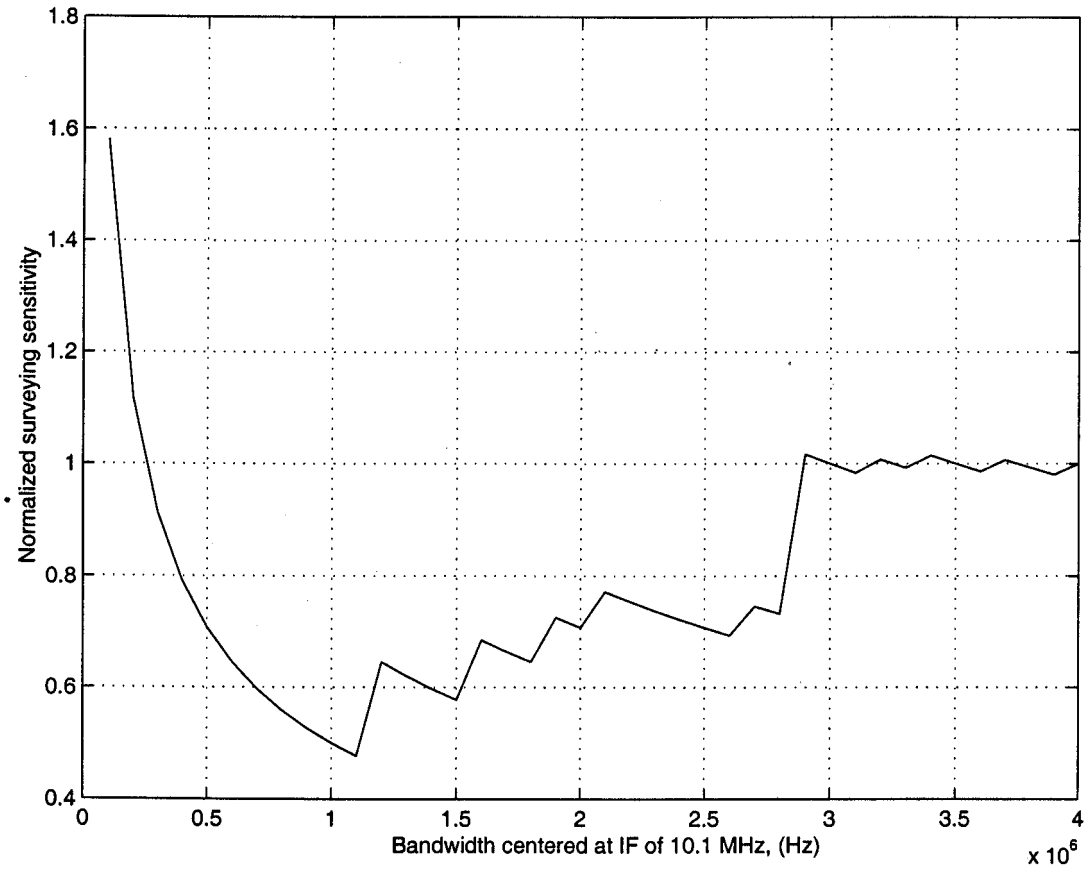

Figure 3.6: Normalized surveying sensitivity using different bandwidths to image $-70° \leq \delta \leq -10°$ with a 512-channel complex correlator which can work with a maximum clock frequency of 12 MHz.

used for imaging will have a much lower decorrelation in the different delay zones.

3.2.2.2 Choice of sampling frequency

The plots in Figure 3.8 show the allowed sampling frequencies according to different criteria for a band of 1 MHz centered at 10 MHz and sampled by a clock with 25% duty cycle, i.e., every fourth harmonic is suppressed. We see in Figure 3.8(a) the allowed sampling frequency according to the bandpass criterion for a 1 MHz band centered at 10 MHz. Figures 3.8(b) and 3.8(c) show

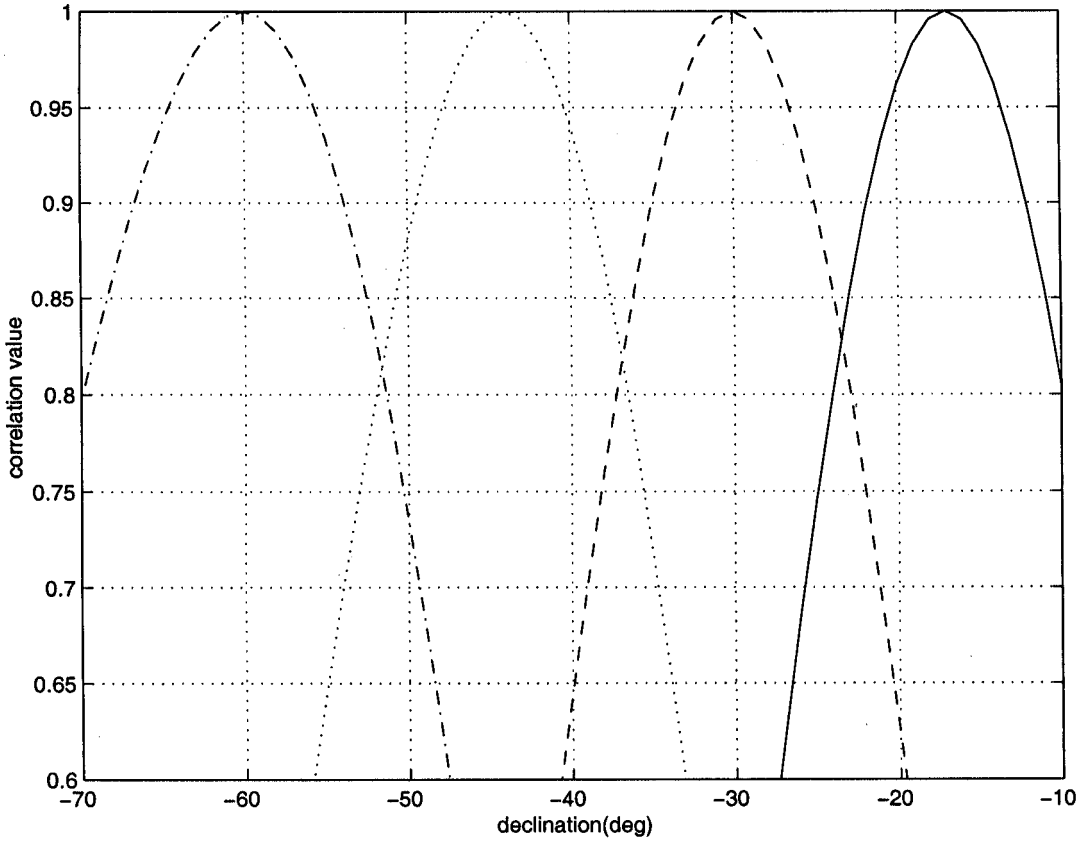

Figure 3.7: Bandwidth decorrelation for a trolley at 880m using a 1 MHz bandwidth with delays compensated for declinations $-17°$, $-30°$, $-44°$ and $-60°$.

the sampling frequencies which do not have harmonics within the 1 MHz band centered at 30 MHz and 151.6 MHz respectively. Figures 3.8(d) shows the maximum frequency usable to be 3 MHz to allow visibility measurements with four delay settings using a correlator that can work up to a clock frequency of 12 MHz. These different criteria are finally ANDed to get the permissible sampling frequencies. Figure 3.8(e) shows the permissible sampling frequencies.

From Figure 3.8(e), we note that there are two permissible frequency ranges. One extends from 2.3333 MHz to 2.3750 MHz and the other from 2.6250 MHz to 2.7143 MHz. To get better sensitivity we chose a frequency

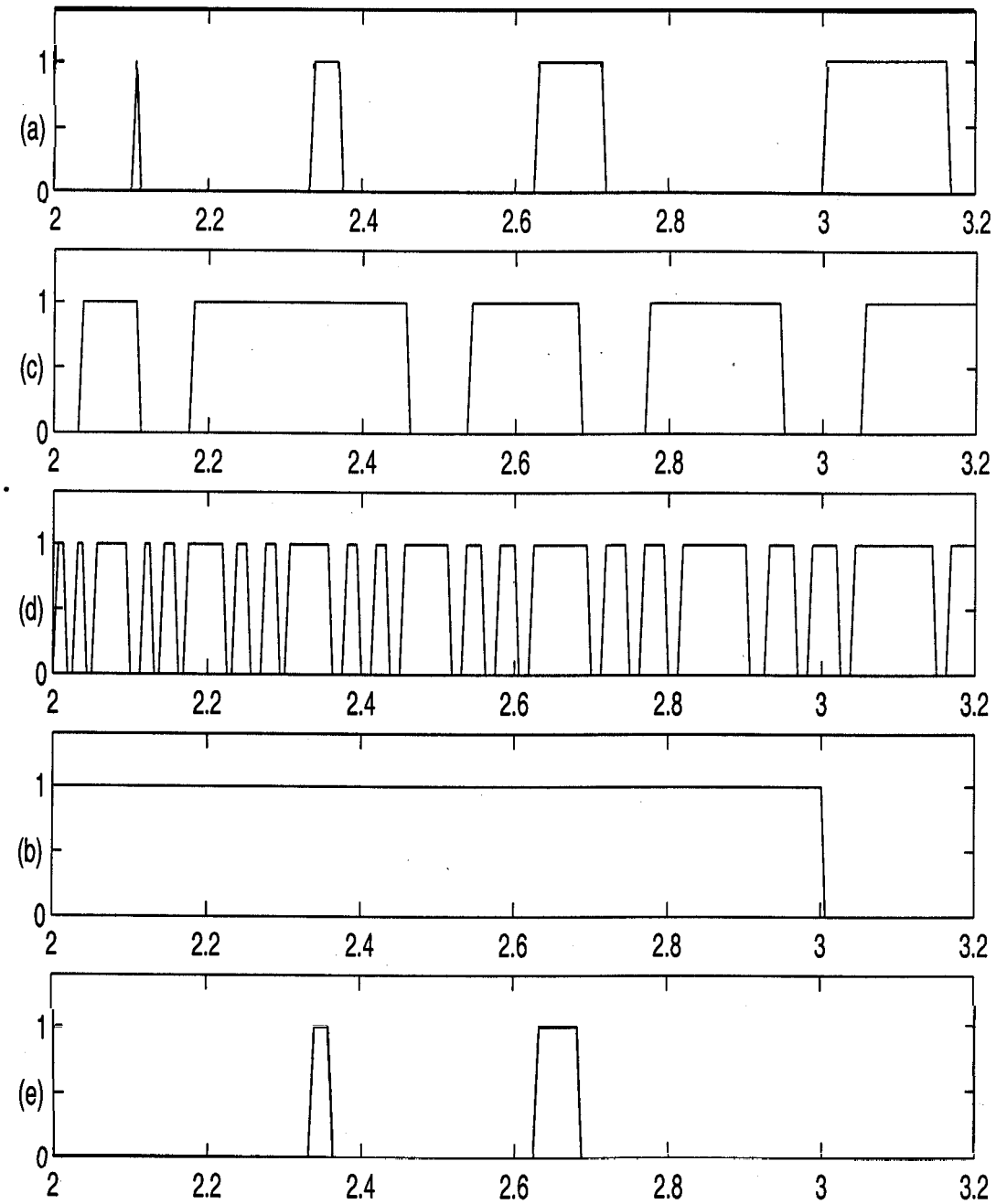

Figure 3.8: The above plots show the allowed sampling frequencies (a) according to the bandpass criterion for a 1 MHz band centered at 10.1 MHz. (b) which do not have harmonics within the 1 MHz band centered at 30 MHz (c) which do not have harmonics within the 1 MHz band centered at 151.5 MHz (d) for recirculating the data 4 times for the four delay zones using a 12 MHz correlator system (e) obtained after ANDing (a), (b), (c) and (d)

in the higher band, i.e., in the range 2.6250 MHz - 2.7143 MHz. We finally chose a sampling frequency of 2.65625 MHz which is almost at the center of this allowed range of frequencies.

3.2.2.3 Choice of memory size

We now consider the options in the implementation of a recirculator system for the MRT. The major factors which influenced the design are

(a) The parameters of the existing correlator system.

(b) The time required for the implementation of a design option

The details of the correlator system are given in Chapter 2 and we discuss here, briefly, the features of the correlator system that affect the design. To keep the cost of the proposed system down, we had aimed to use minimal external memory which was the most expensive component.

1. The correlator chips VLA-1 and VLA-2 have a fixed integration period of 2^{13} clock cycles, i.e., 8 K clock cycles. Therefore to recirculate data, we need an external storage of two banks of memory each of size at least 8 K. The integrated correlations resulting from the 8 K samples have to be stored on the RAM (random access memory chip) on the correlator board for the four delay settings.

   There are 17 correlators on each correlator board which also has a dual-memory buffer, each of size 128 bytes (a total of 256 bytes). Of these, only 68 bytes[g] are used for storing the correlation values of the 17 correlators. For storing correlation values corresponding to 4 delay settings, we would need four times this size, i.e., 68 x 4 = 272 bytes. The memory chips

[9] $17(correlators) \times 2(bytes/correlator) \times 2(banks) = 68\ bytes.$

provided on the correlator boards have only 256 bytes. We therefore need to rewire a larger RAM in place of the existing one.

In this option, we need to employ an external RAM of size 8 K×2 and need to modify the correlator boards to have enough memory for storing the correlation values for all the delay zones. We also need to reprogram the on-board PROMS to allow for addressing a larger RAM. This option would require rewiring of all the 64 correlator boards. Since the correlator boards are four layered boards, the rewiring process is rather complex.

2. The memory requirement could be reduced if we reduce the number of correlations by combining the east-west groups, i.e., by making each east-west group 128 m wide instead of 64 m. Then there will be only 16 east-west groups instead of the existing 32. The number of correlations are then brought down to 9 per board and the memory required on the correlator board for storing the correlation values for the 4 delay zones is 144 bytes[10]. This amount of memory is available on the RAM and therefore eliminates any rewiring of the correlator boards. This option requires an external RAM of size 8 K x 2 and also requires reprogramming the on-board PROMS.

   In this option, we need to combine EW groups to make them 128 m wide instead of 64 m. This is not possible because we do not always have 2 groups which are at the same height and are adjacent to one another. To combine non-adjacent groups at the same height would require our local-oscillator distribution to be redone so that the LO in the two groups being combined are always synchronized with zero-phase difference. We could have combined groups of different sizes to get 16 final groups in

[10] $(8+1)(correlators) \times 2(bytes/correlator) \times 2(banks) \times 4(zones) = 144\ bytes.$

the east-west arm. However, groups of different sizes will have different primary beamwidths. This would prevent us from doing two-dimensional synthesis in the future.

3. Since the size of the memory available on the correlator boards is not enough to take care of the 4 delay zones, it is necessary to transfer the integrated correlation value of each zone to an external memory and then process the other delay zone. The size of the external RAM would be determined by the minimum integration period required on the correlator boards. However if one chooses the minimum integration time possible, one has to ensure that data can be transferred out of the correlator boards at the fast rate required.

   Data is integrated for 2^{13} clock cycles in the VLA-2. In the existing system, data from the VLA-2 is further integrated on the on-board RAMs for a minimum of $2^4 = 16$ such pre-integration's cycles. If one wants to reduce this to say $2^3 = 8$ pre-integration cycles, then the external memory required would be

$$2^{13}(\text{VLA} - 2\ \text{integration}) \times 2^3(\text{post} - \text{integrations}) = 64\ \text{K/channel/bank}$$

   This option requires the correlator system to put out 1088 words in about 5.5 ms[11]. The correlator system at present can put out 1088 words in about 11 ms[12].

   Therefore the minimum post-integration has to be $2^4 = 16$ pre-integration

[11] $2^{13} \times 2^3$ clock cycles at **12 MHz** $\approx$ **5.5** ms
[12] $2^{13} \times 2^4$ clock cycles at **12 MHz** $\approx$ **11** ms

cycles. This option requires an external RAM of:

$$2^{13}(\text{VLA} - 2\ \text{integration})\ \text{x}\ 2^{4}(\text{post} - \text{integrations})$$
$$= 128\ \text{K/channel/bank}$$

This requires a data acquisition system that can pick up data at the rate of 1088 words in 11 ms.

The recirculator design using external dual memory buffers each of 128 K/Channel/bank was undertaken because this option required minimal modifications to the existing system.

3.2.2.4 Design criteria for a Data Acquisition System (DAS)

The specifications of the data acquisition system and a few design constraints are listed below

- It should be able to acquire 1088 correlation values every 11 ms. The acquisition cycle has the following steps: The DAS has to send the correlator number from which the data has to be acquired, followed by the control signal called data accept (DA), to latch the correlator number. The correlator responds with the RDY signal once the correlator value is available on its output bus. The RDY signal should be polled by the DAS and when found active, the data should be acquired.

- It should read the sidereal time information from the astronomical clock to time-stamp the data. The time-stamp information is 4 bytes long. A separate I/O port is required for reading the time information.

- It should be able to program the correlator system and update it every 11 ms.

- It should be able to post-integrate the acquired data to about 1-second packets and transfer the data onto a hard drive.
- The system should be robust and be capable of running continuously for many days.
- The design should preferably be PC based. A PC based system requires lesser design and implementation time.
- The data acquisition software should be written in C and assembly language.

  At the MRT site, 80386 PCs with ISA bus were readily available. Using a single PC, we were not able to complete all the steps of acquisition such as programming the delays every 11 ms, acquiring the 1088 words of correlation values, integrating them, acquiring the time information and then writing to the hardrive once every second. Therefore a data acquisition system employing a dual memory buffer shared by two 80386 PCs running on DOS were used. While one PC acquires and integrates the data onto one bank, the other PC has enough time to transfer the data to the hardrive.

3.2.3 Hardware description

The recirculator system is designed as a modular system consisting of several identical recirculator boards and a central control board for the generation of control signals. These are distributed by a set of driver boards to the individual recirculator boards. The recirculator boards are designed around the MCM6902 memory chips, each of size 64×4, with an access time of 25 ns. Eight such chips along with the control logic could be placed on a double sided PCB

of a reasonable size, and therefore, each recirculator board caters for 4 channels (each channel has 2 bit/sample). The total number of channels is 16 for the east arm, 16 for the west arm and 16 x 2 for north-south arm, i.e., 64 channels in all. Since each board caters to 4 channels, we require 16 recirculator boards. However, to maintain the flexibility of switching to the Pencil beam mode, EW x NS, and Fan beam modes, EW x E and (NS+W) x NS, four additional boards were employed to provide the 16 Sin channels for the east groups.

The block diagram of a recirculator board is shown in Figure **3.9.** The digitizer (sampler units) outputs are ECL compatible. However, for reasons of power consumption and availability of memory chips, the recirculator logic is TTL based. Therefore, at the input of each recirculator board, the data from the samplers are converted from ECL levels to TTL levels. This data is then resampled using a latch with a programmable 'resampling clock'. The resampled data is written into one bank of the RAM. The RAMs are addressed by 17 bit counters which are clocked by a slow clock for write operations and a fast clock for read operations. While the data is being written on one bank of the RAM slowly, the other RAM bank is being read out at a fast rate. The data read out is again converted to ECL levels to make them compatible with the data input to the correlator boards. The data is read out a number of times depending on the number of zones being processed.

The recirculator boards have the facility to select :

1. The number of delay zones. These are programmable to **2, 3,** or 4 zones. This simultaneously selects the resampling frequency and the integration period.

2. Operation in bypass mode: the data in this mode does not go through the memory of the recirculator.

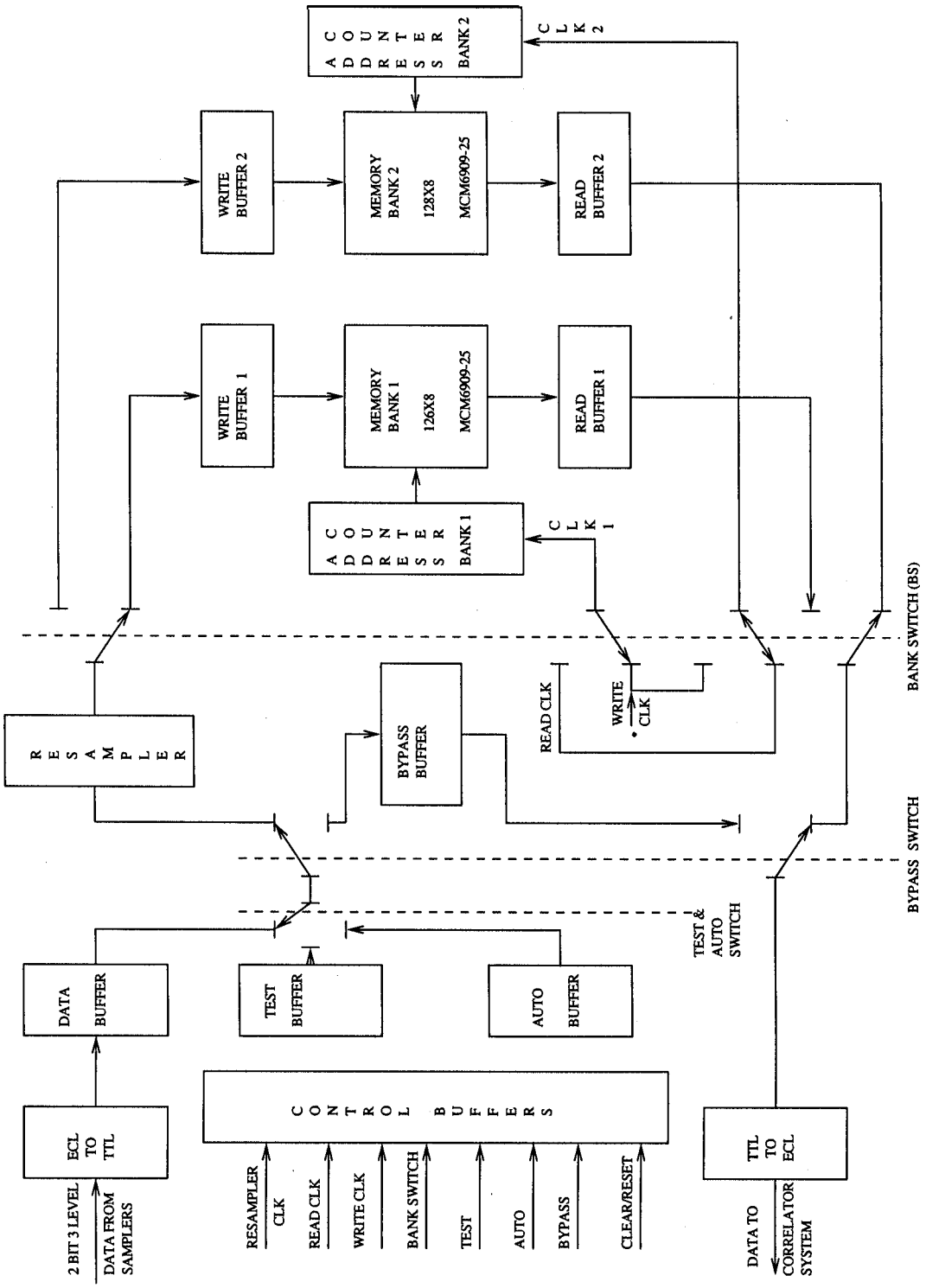

Figure **3.9:** Block diagram of the MRT recirculator board.

3. Operation in test mode: In the test mode, test data may be introduced into the recirculator system to test the working of an individual recirculator board. Test data is introduced through the test-buffer on the recirculator boards.

4. Operation in autocorrelation mode: This mode allows the correlator system to be used as a 128 channel auto-correlator directly and with some additional hardware, we can use it as a 4096 channel auto-correlator using the recirculator. The data for the autocorrelation is introduced through the auto-buffer on the recirculator boards.

   Although the Autocorrelation and Test mode features have been provided in the recirculator boards, the rack has not been wired for use in these modes.

3.2.4 Data acquisition system for the recirculator.

The block diagram of the control and data acquisition system is shown in Figure 3.10. The two PCs used are referred to as PC1 and PC2. PC1 communicates with the correlator system. It sends the control signals to configure the correlator for different modes of operation (Section 2.2.2) and programs the delays in the correlator system. It also collects the data from the correlator system and integrates onto a double bank memory. The data for different zones are acquired onto different sections in the memory bank, with each zone alloted $(17+1)\times 64\times$ *Number of bytes per correlation.* The extra 64 x *Number of bytes per correlation* are kept to store any other information related to the data, e.g. time stamps. PC1 reads the sidereal time from the astronomical clock and time-stamps the acquired data. At the end of each one-second integration, PC1 swaps the banks and sends an interrupt to PC2. While PC1

continues acquiring data and integrating onto the second memory bank, PC2 picks up the data from the first memory bank and transfers them over a point-to-point Ethernet network onto a hardrive of a Linux-based PC, which is a part of the Local Area Network (LAN) connecting other machines through a gateway. A data file is opened for writing and is closed at the end of each integration. This prevents loss of data if there is a power failure which causes the data acquisition to stop. Having a separate network for the acquisition system ensures a reliable transfer of data and any fault or breakdown in the LAN connecting other machines does not affect the acquisition of data. Furthermore, data checking, processing of the acquired data, and data backup[13], can be done simultaneously without affecting the data acquisition. Using the newly designed DAS, acquiring the 1088 words of data from the correlator system to PC1, integrating them and programming the correlator system with the new delays could be carried out in 11.62 ms.

In the recirculator mode, with the sampling frequency at 2.65625 MHz, the maximum/minimum correlation count for one second integration is ±179256, This requires 19 bits of data storage memory per channel (data is pre-integrated for 2^{17} clock cycles in the correlator boards and then further integrated 22 times in the DAS to get about 1 s packets). However, no celestial source in our beam (not even the Sun) is expected to produce a correlation count to fill a 16 bit counter, i.e., ±32768 for an integration of about 1 s . This value corresponds to a normalized correlation coefficient of about 0.2 (i.e., $\rho \approx 0.2$). Therefore, it suffices to record only two bytes of data for each correlation value of 1 s integration. Generally, only interference is expected to cause an overflow of this two byte data. If the addition in DAS of pre-integration values causes an over-

[13] data is backed up on 8mm tapes.

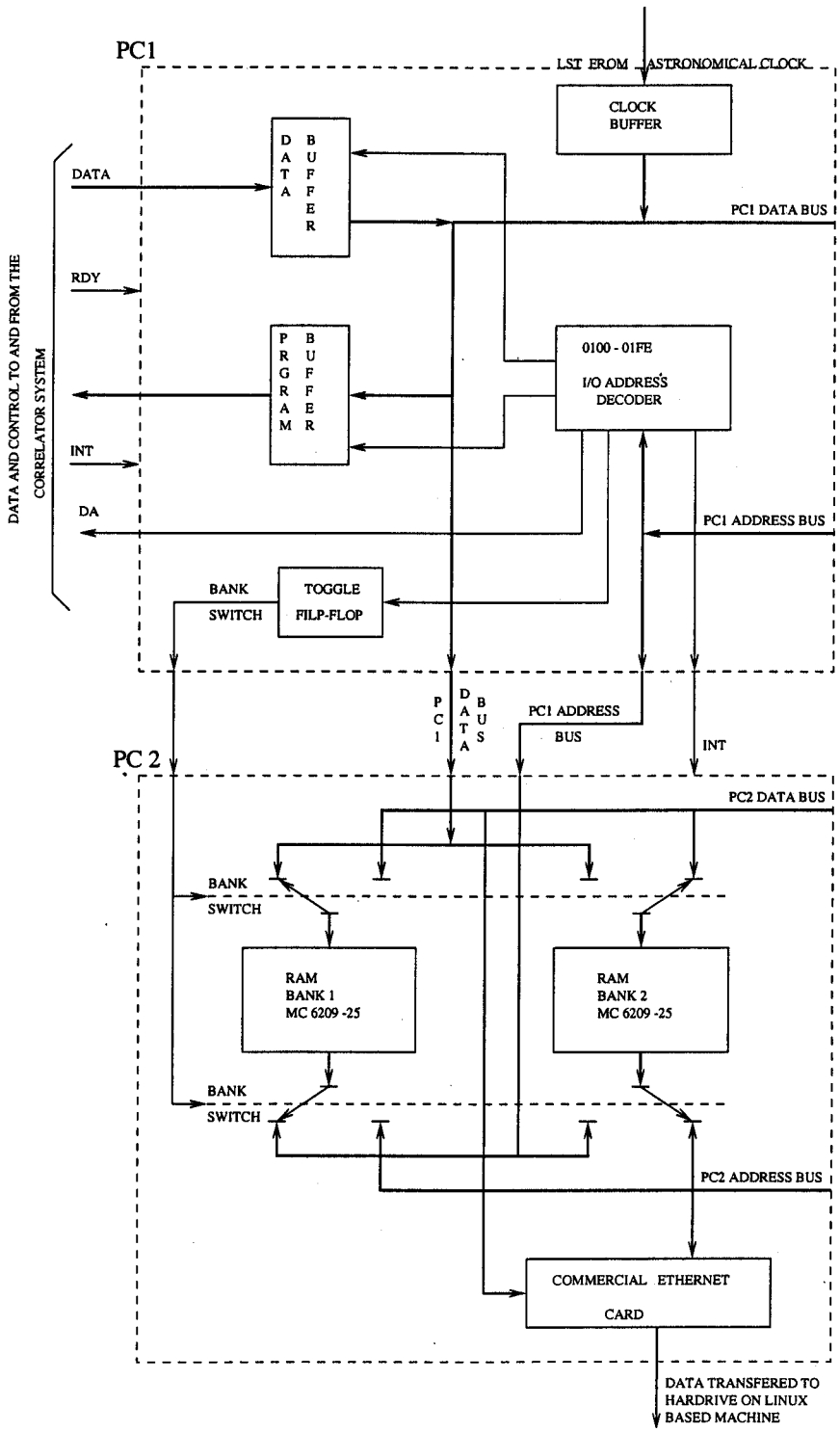

Figure 3.10: Block diagram of the control and data acquisition system.

flow, then this data is not added. This basically results in some interference clipping within the 1 s data.

A self-correlator counts the number of samples which have values between the threshold levels in one pre-integration cycle. In a 2-bit 3-level system with $\frac{V_{th}}{\sigma} = 0.7$, the self correlation value for gaussian signals is about 54% of the maximum correlation counts. This is around 100,000 for the 1 second integration and requires a 17 bit representation. We divide each pre-integrated value of self correlation by 4 before post-integrating on the DAS. This results in an error of about 66 counts which is of the order of 1σ.

It may be recalled (Section 2.2.2) that all but two of the group outputs go through the AGC. The self-correlation outputs of these two channels are used to convert the 2 x 3 digital correlation counts to corresponding analog correlation counts. Although self correlation values are plagued with local pickup, the two non-AGC channels used for estimating total power are stored separately as 4 byte data each to avoid any deterioration in the estimation of total power due to clipping.

After every 49.34 ms of integration (2^{17} clock cycles at 2.65625 MHz), data from the correlator boards for the 4 delay zones are transfered and integrated on the DAS to build 1.0856 s (22 integrations) data packets. These are transferred to the hard-drive over the network. Thus every second we store 9216 bytes[14] of data resulting in about 760 MB of data for a 24 hour observation.

To facilitate data handling and automation of data processing, the data is organized in hourly (LST) files. The allocation, the LST hour and the Julian Day are encrypted in the name of the observation file.

[14] $(17+1)\times 64$ **(boards)x 4 (delay zones)x** 2 (bytes/sample) $=9216$

3.3 System tests

The recirculator system has a test mode (Section 3.2.3). However, since the rack was not wired for this mode, the signals for testing were fed through the data buffer. In the first stage of testing, the complete system was debugged using static inputs. After initial debugging, tests were then carried out by feeding carrier wave and noise signals as inputs. Finally, data on actual observations of MRC 1932-464 were used to compare the recirculated data with that obtained without the recirculator. The delays were identical in the two cases and the only change in S/N expected was that due to the reduced sampling from 12 MHz to 2.65625 MHz which is of the order of 10%. For comparison, we generated the RA scan on MRC 1932-464. The RA scan was obtained by phasing the response of all the 480 NS×EW baselines measured on a single day to the declination of MRC 1932-464.

Figure 3.11 shows the RA scans of the calibrator obtained with and without the recirculator. The fourier transforms of these scans are shown in Figure 3.11b. We compared the noise in the Fourier domain[15] where we can easily get an estimate of the RMS variations from the receiver by measuring the noise beyond the frequency up to which there is contribution from celestial sources. We found the deterioration in the signal-to-noise ratio due to the recirculator to be less than 10%.

After being satisfied with a 1D scan on one allocation, we used the complete data of block-3 (172 m - 261 m) to make a 2D image around MRC 1932-464. Block-3 has 6 allocations of the 15 trolleys. We ascertained the quality of data in each one of the allocations by checking the RA scans of each allocation.

[15] Fourier transform of the RA scan nicely separates the contribution from the sky with the receiver noise and the receiver noise alone. At frequencies above $\frac{1}{16}$ Hz we will have only the receiver noise.

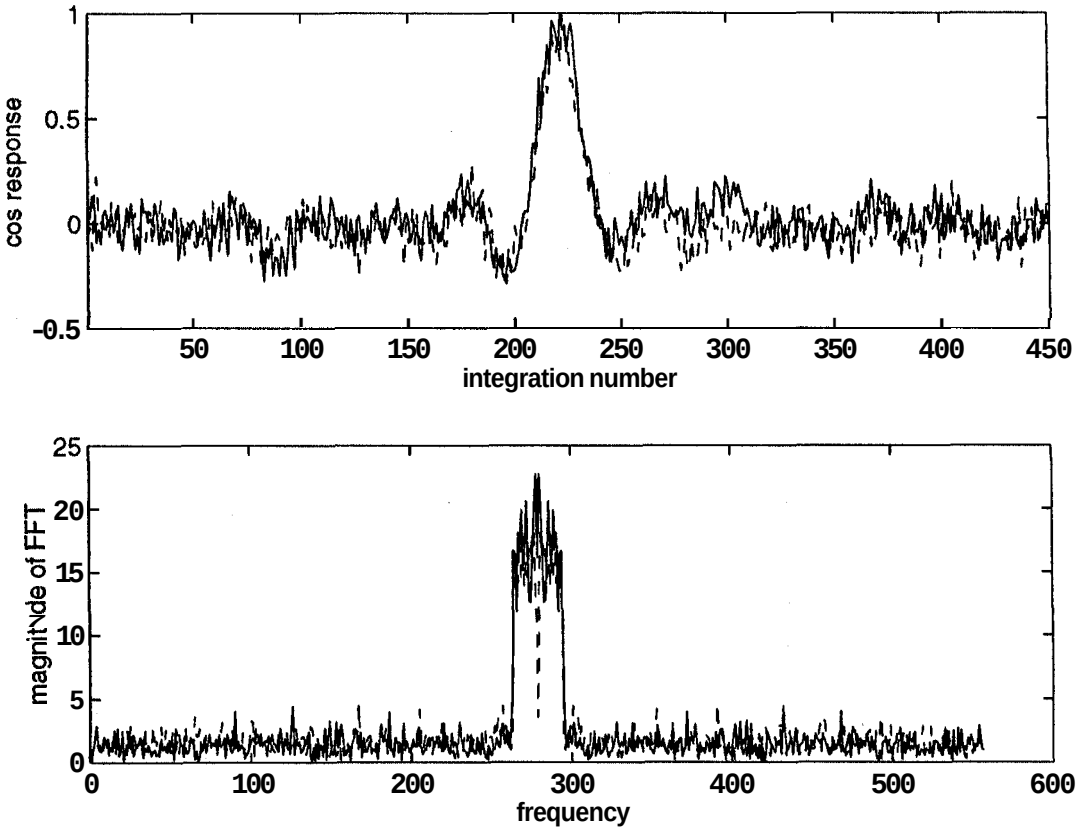

Figure **3.11:** Comparison of RA scans of MRC **1932-464** with the recirculator system (dashed line) and without the recirculator system (solid line) (a) in time domain (b) in frequency domain.

The RA scans on MRC **1932-464** for each of the six allocation are shown in Figure **3.12.** These were found to be comparable to each other and to those obtained without the recirculator.

The images of these six allocations were added and the final image is shown in Figure **3.13.** Since the image uses visibilities on north-south baselines from **172** m, the beam has very high sidelobes. A cut at the declination at the transit was compared with the expected beam-shape and is shown in Figure **3.14.** They are seen to agree very well with each other. The skewness seen in the beam is due to the non-coplanarity of the array and is explained in Chapter 5.

These tests and comparisons indicated the success of the hardware systems

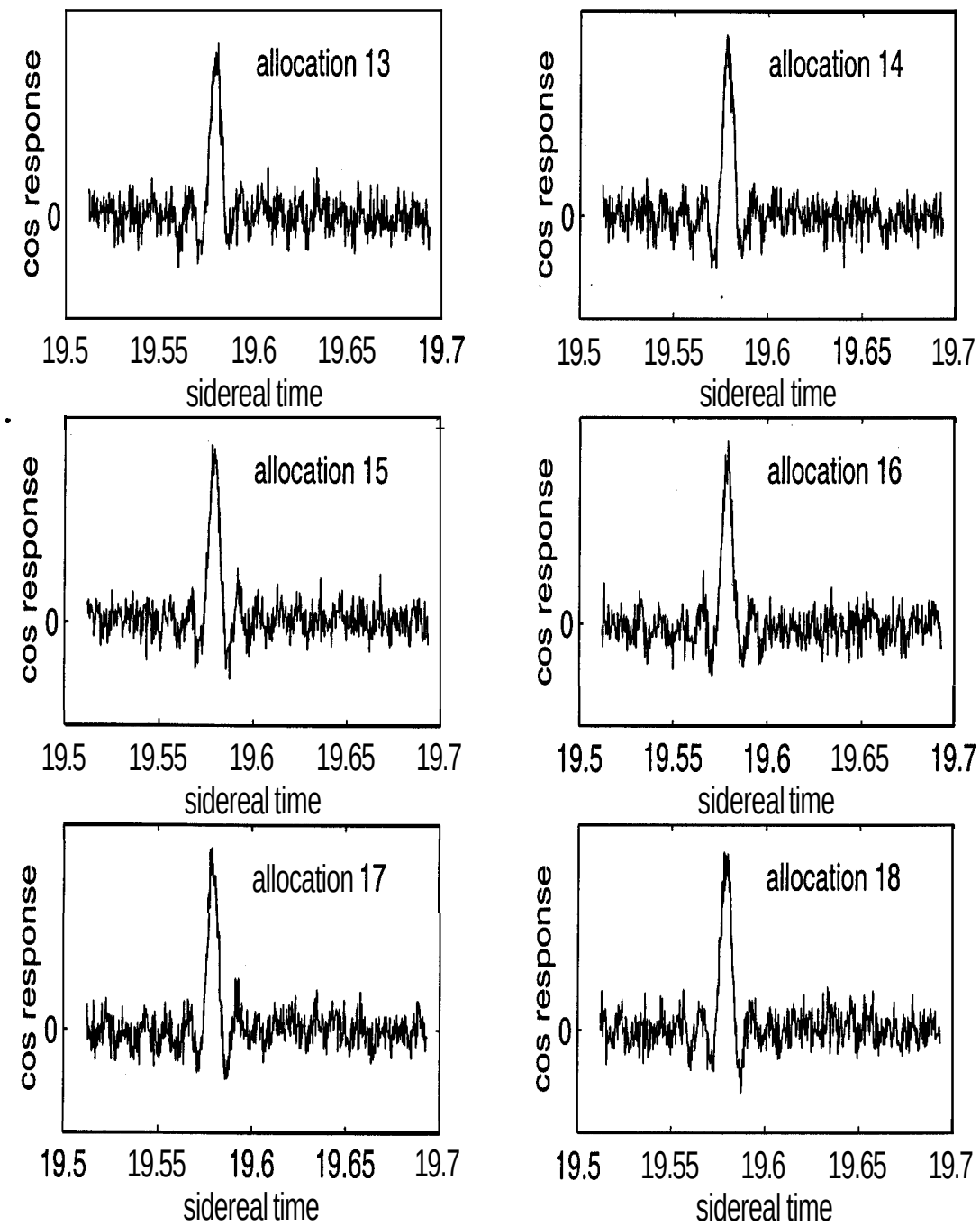

Figure 3.12: RA scans on MRC 1932-464 for each allocation used in making the map.

developed.

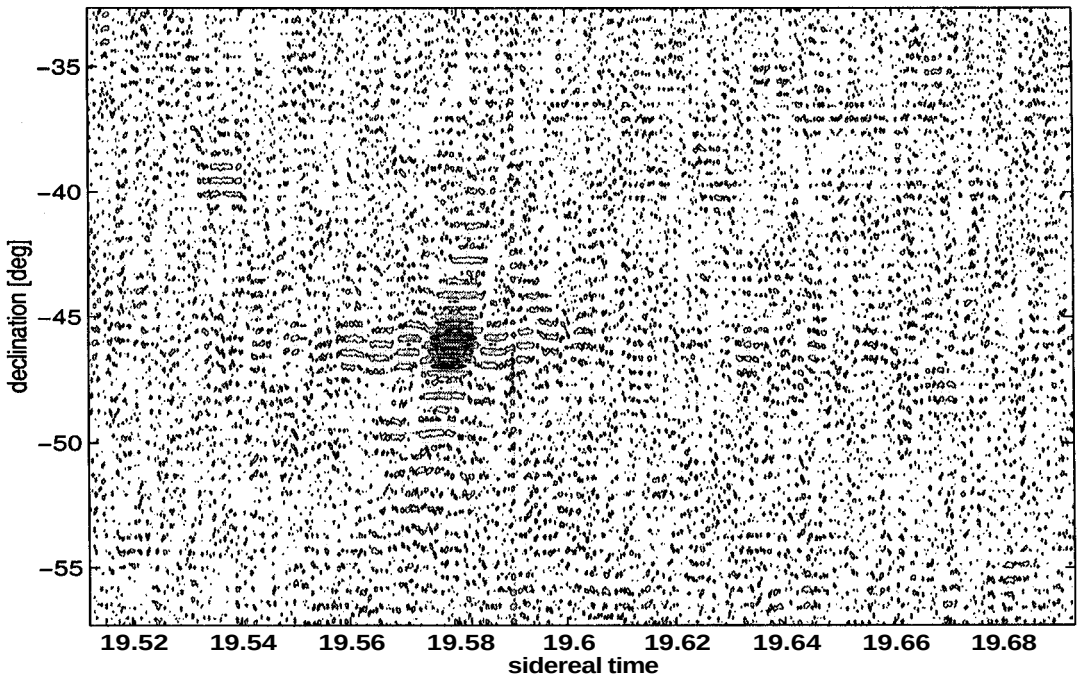

Figure 3.13: Image of the region around MRC 1932-464 made by combining data of allocation 13 to allocation 18 (block-3).

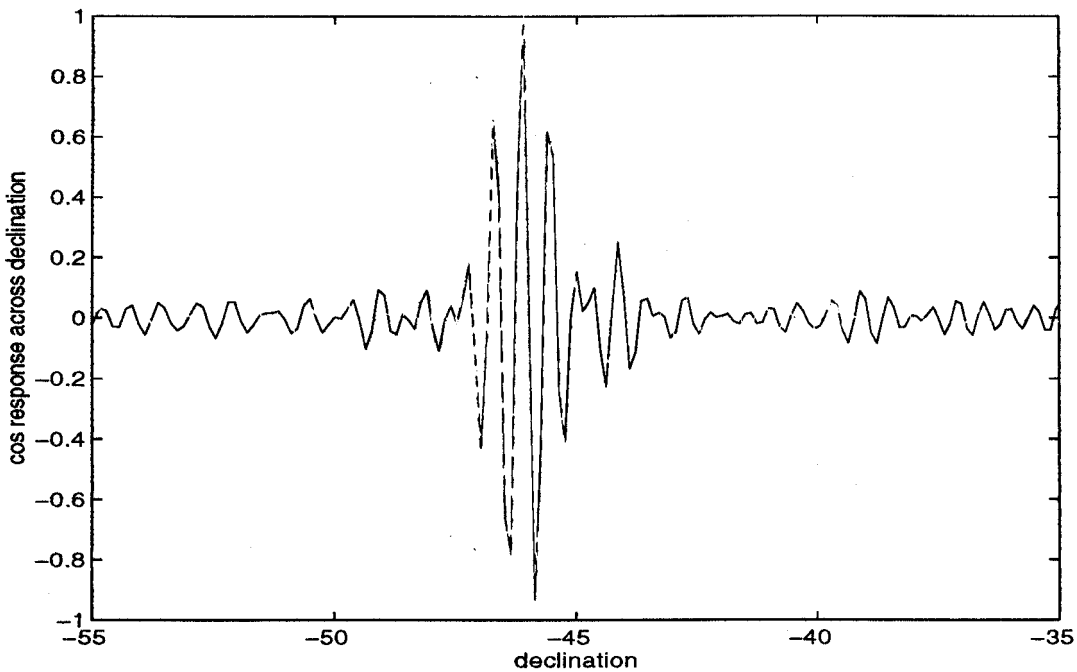

Figure 3.14: Comparison of beam in declination of MRC 1932-464 (solid line) with the expected response ignoring the height effect (dashed line).